Arteriosclerosis, Thrombosis, and Vascular Biology
Volume 40, Issue 1, January 2020; Pages 239-254
https://doi.org/10.1161/ATVBAHA.119.313506

TRANSLATIONAL SCIENCES

Extracellular Vesicles From Adipose Stem Cells Prevent Muscle Damage and Inflammation in a Mouse Model of Hind Limb Ischemia

Role of Neuregulin-1

Federico Figliolini, Andrea Ranghino, Cristina Grange, Massimo Cedrino, Marta Tapparo, Claudia Cavallari, Andrea Rossi, Gabriele Togliatto, Saveria Femminò, Maria Vittoria Gugliuzza, Giovanni Camussi*, and Maria Felice Brizzi*

OBJECTIVES: Critical hindlimb ischemia is a severe consequence of peripheral artery disease. Surgical treatment does not prevent skeletal muscle impairment or improve long-term patient outcomes. The present study investigates the protective/regenerative potential and the mechanism of action of adipose stem cell-derived extracellular vesicles (ASC-EVs) in a mouse model of hindlimb ischemia.

APPROACH AND RESULTS: We demonstrated that ASC-EVs exert a protective effect on muscle damage by acting both on tissue microvessels and muscle cells. The genes involved in muscle regeneration were up-regulated in the ischemic muscles of ASC-EV-treated animals. MyoD expression has also been confirmed in satellite cells. This was followed by a reduction in muscle function impairment in vivo. ASC-EVs drive myoblast proliferation and differentiation in the in vitro ischemia/reoxygenation model. Moreover, ASC-EVs have shown an anti-apoptotic effect both in vitro and in vivo. Transcriptomic analyses have revealed that ASC-EVs carry a variety of pro-angiogenic mRNAs, while proteomic analyses have demonstrated an enrichment of NRG1 (neuregulin 1). A NRG1 blocking antibody used in vivo demonstrated that NRG1 is relevant to ASC-EV-induced muscle protection, vascular growth, and recruitment of inflammatory cells. Finally, bioinformatic analyses on 18 molecules that were commonly detected in ASC-EVs, including mRNAs and proteins, confirmed the enrichment of pathways involved in vascular growth and muscle regeneration/protection.

CONCLUSIONS: This study demonstrates that ASC-EVs display pro-angiogenic and skeletal muscle protective properties that are associated with their NRG1/mRNA cargo. We, therefore, propose that ASC-EVs are a useful tool for therapeutic angiogenesis and muscle protection.

Key Words: endothelial cells ■ ischemia ■ myoblasts ■ neuregulin-1 ■ proteomics

Correspondence to: Maria Felice Brizzi, Department of Medical Sciences, University of Turin, Corso Dogliotti 14, 10126, Turin. Email mariafelice.brizzi@unito.it
Giovanni Camussi, Department of Medical Sciences, University of Turin, Corso Dogliotti 14, 10126, Turin. Email giovanni.camussi@unito.it
* These authors contributed equally to this article.
For Sources of Funding and Disclosures, see page 253.

The online-only Data Supplement is available with this article at https://www.ahajournals.org/doi/suppl/10.1161/ATVBAHA.119.313506.

Nonstandard Abbreviations and Acronyms

ASC-EVs	adipose stem cell-derived extracellular vesicles
BrdU	5-bromo-2-deoxyuridine
EGR1	early growth response 1
HMEC	human microvascular endothelial cells
I/R	ischemia/reperfusion
Myf5	myogenic factor 5
MyoD	myoblast determination protein 1
NRG1	neuregulin 1
p38MAPK	P38 mitogen-activated protein kinase
Pax7	paired box protein 7
SCs	satellite cells

Highlights

- Adipose stem cell-derived extracellular vesicles prevent muscle damage after acute hindlimb ischemia.
- Adipose stem cell-derived extracellular vesicles induce vascular growth and protect muscle against ischemia/reperfusion damage.
- Adipose stem cell-derived extracellular vesicles are enriched in NRG1 (neuregulin 1) and pro-angiogenic mRNAs.
- Adipose stem cell-derived extracellular vesicles via NRG1 impair inflammatory cell infiltration in muscles subjected to ischemia/reperfusion.

Critical limb ischemia is a widespread disorder caused by the atherosclerosis of the peripheral arteries and is commonly found in patients with peripheral artery disease.[1] Reduced blood supply to the ischemic limb leads to skeletal muscle damage. The standard therapies, which are surgery and endovascular intervention, are not particularly effective, making patient management a significant economic burden.[2,3] The exponential growth of an aging population, the onset of diabetes mellitus, and the high incidence of metabolic disease also pose a heavy social encumbrance but are also driving forces for novel and effective therapeutic options. Regenerative medicine and in particular cell-based therapy, has recently gained a great deal of attention.[4] Mesenchymal stem cells, derived from a variety of sources, have been proposed to fulfill this role.[4] Bone-marrow derived mesenchymal stem cells are currently the most widely studied stem cells in regenerative medicine as they are known to home in and engraft injured tissues. However, special clinical interest has recently been shown in the use of adipose-derived stem cells (ASCs) in the ischemic setting as a range of useful properties, such as stimulation of angiogenesis, muscle regeneration and inflammation suppression,[5] have been attributed to them. Moreover, compared with mesenchymal stem cells, ASCs could be easily obtained. However, the inefficient engraftment

of mesenchymal stem cell and ASC suggests that their positive effects depend on their secretome (paracrine/autocrine hypothesis).[6]

Stem cell-derived extracellular vesicles (EVs) have emerged over the past decade in their role as important mediators of intercellular communication; they are involved in the transmission of signals between cells to regulate a wide range of biological actions.[7] Significant insight into the functional role that they play in a number of clinical settings has been gained.[7] In particular, it has been found that stem cell-derived EVs can mimic the effect of the cell of origin via the horizontal transfer of functional RNAs and proteins when systemically or locally administrated in regenerative medicine. The use of EVs for genetic information transfer has, therefore, also been proposed.[8] EVs that are released from stem cells can drive regenerative programs in cells that have survived injury in various pathological settings, such as heart ischemia/reperfusion (I/R) injury,[9] and hepatectomy[10] models. miRNAs, mRNAs, and proteins carried by EVs have been proven to favor angiogenesis and tissue regeneration.

Skeletal muscle damage is a hallmark of persistent (I/R) injury in patients with atherosclerosis of the peripheral arteries. In response to skeletal muscle damage, resident stem cells, known as satellite cells (SCs), are recruited and promptly participate in the regenerative processes by undergoing cell division. Myogenic regulatory factors Myf5 (myogenic factor 5) and MyoD (myoblast determination protein 1) are specific markers of the participation of differentiating myoblasts in the complex network of events during myogenesis.[11] However, tissue recovery after damage also requires an efficient blood supply, which is impaired in acute I/R injury. The pro-angiogenic properties of ASC-derived EVs have been reported to mainly depend on their miRNA cargo.[12] The present study investigates whether ASC-derived EVs may act on both vascular and skeletal muscle cells to protect muscles upon acute I/R damage and by which mechanism this may occur.

MATERIALS AND METHODS

The authors declare that all supporting data are available within the article and in the online-only Data Supplement.

In Vivo Model of Hindlimb Ischemia

Animal studies were conducted in accordance with the Italian National Institute of Health Guide for the Care and Use of Laboratory Animals. All procedures were approved by the Ethics Committee of the University of Turin and the Italian Health Ministry (authorization number: 490/2015-PR). Mice were housed according to the Federation of European Laboratory Animal Science Association Guidelines. All experiments were performed in accordance with relevant guidelines and regulations. C57BL/6J male mice (Charles River Laboratories), aged 7 to 8 weeks were used. Since the female estrus cycle could introduce unexpected variables, only male mice have been used in this study. Hindlimb ischemia was performed as previously described.[13,14] Two different ASC-EV administration routes were used in the preliminary study: route 1, ASC-EVs (2×10^{10}/mouse) were injected as detailed: 1×10^{10} administrated intravenously immediately after intervention (T0), 0.5×10^{10} via intramuscular injection on day 1 (T1) and again on day 2 (T2); route 2, ASC-EVs were injected intramuscularly at 1×10^{10} immediately after surgery (T0), and at 0.5×10^{10} at day 1 (T1) and day 2 (T2; n=8/each group/protocol). Animals were euthanized on either day 3 (T3) or day 7 (T7) for molecular and histological analyses (n=8/group). In selected

experiments, ASC-EVs pretreated with a blocking antibody against NRG1 (neuregulin 1; Raybiotech) were used (n=8). Semi-quantitative estimations of foot damage[15] (by repeated measures, analyzed using the ANOVA and Newman-Keuls Multiple Comparison tests) of foot damage were performed serially using the following classification: 3=dragging of foot (foot necrosis); 2=no dragging, but no plantar flexion (foot damage); 1=plantar flexion, but no toe flexion (toe damage); and 0=flexing the toes to resist gentle traction on the tail (no damage).[15] To monitor blood flow, mice were placed on a heating plate at 37°C for 5 minutes, after anesthesia, to minimize temperature variations. Hindlimb blood flow was measured using a Laser Doppler Blood Perfusion analyzer (PeriScan PIM 3 System, Perimed, Stockholm, Sweden), immediately before and after surgery, and at days 3 and 7 after surgery. Laser Doppler Blood Perfusion analysis was performed on hind limbs and feet. Blood flow was reported as changes in the laser frequency, using several color pixels. Images were analyzed to quantify blood flow using regions of interest that were drawn freehand. Hindlimb blood flow was expressed as the ratio of left (ischemic) to right (nonischemic) to avoid data variations that may be caused by ambient light and temperature.[13] To assess the area of muscle damage, at day 7 muscles were rapidly removed and incubated for 20 minutes at 37°C in 0.1% solution of nitro-blue tetrazolium in phosphate buffer. The necrotic mass was expressed as a percentage of total muscle mass (n=4 each/group protocol).[16] Details are reported in the online-only Data Supplement.

Histological and Immunofluorescence Analyses

Gastrocnemius muscle sections from ischemic and normo-perfused limbs were stained with hematoxylin and eosin and Masson's trichrome for histological analysis. Images of all the injured areas of the ischemic limb sections were acquired for total muscle fiber counts. Random images from total nonischemic limb sections were used as controls. Data were quantified as percentage of damage area over total area. Capillary density was calculated as the number of capillaries per muscle fiber in Masson's trichrome sections. Ten randomly chosen microscopic fields, from 3 different sections in each tissue block, were examined and counted by 2 blind observers using Image J software. Capillary density was expressed as the number of capillaries per muscle fiber±SEM (magnification, ×400). Inflammatory cells in gastrocnemius muscles were quantified using immunofluorescence analyses on optimal cutting temperature compound embedded samples. Tissue slices (5 μm) were stained with a rat anti-mouse CD14 primary antibody (PharMingen). Fifteen randomly chosen microscopic fields, from 3 different sections in each tissue block, were examined for inflammatory cell count (2 blind observers). Inflammation was expressed as the number of CD14 positive cells per high power field±SEM (magnification, ×400).

Muscle cell proliferation was evaluated by immunohistochemistry. Gastrocnemius muscle sections (paraffin-embedded samples) were stained with a monoclonal anti-proliferating cell-nuclear antigen-antibody (Santa Cruz; at day 7). Apoptosis was evaluated using the TUNEL (terminal deoxynucleotidyl transferase dUTP nick-end labeling) assay (ApopTagOncor, Gaithersburg, MD). Number of proliferating cell-nuclear antigen-positive cells and TUNEL-positive nuclei were evaluated by counting the number of positive nuclei per field in 10 randomly chosen sections using ImageJ software. Details are reported in the online-only Data Supplement.

Isolation and Characterization of ASC-EVs

Male-derived ASCs were purchased from Lonza and cultured in ADSC growth medium (Lonza) in T75 flasks. For EV isolation, ASCs (passage 2–7 and 60%–70% of confluence) were washed several times with PBS (Lonza), to eliminate traces of serum and then cultured in alpha MEM

(Lonza) with penicillin/streptomycin and L-glutamine (Sigma-Aldrich, St Louis, MO) without FBS overnight (16 hours) in 5% CO_2 incubator at 37°C. Cell culture supernatants (8 mL each T75 flask) were centrifuged twice at 4000 rcf, for 10 minutes, at 4°C and submitted to microfiltration (0.22 µm PES from Meck Millipore, Tullagreen, Ireland) to eliminate cell debris and apoptotic bodies, and then ultracentrifuged at 100 000 rcf, for 2 hours, at 4°C in a Beckman Coulter Optima L-90K ultracentrifuge with rotor 70 Ti in polycarbonate tubes (355618; Beckman Coulter, Indianapolis, IN). Pellets were resuspended in alpha MEM supplemented with 1% DMSO and stored at −80°C for further experiments. In selected experiments, ASC-EVs were either treated with anti-NRG1 blocking antibody (Raybiotech) 5 µg/mL for 1 hour at RT, or with trypsin 0.1X (0.025% w/v) for 1 hour at 37°C, then washed with PBS, re-ultracentrifuged at 100 000 rcf for 2 hours, at 4°C and resuspended, as previously described.[13]

To perform Nanosight Tracking Analyses, ASC-EVs were diluted (1:200) in sterile saline solution (NaCl 0.9%) filtered with 0.1 µm pore filter and analyzed using a NanoSight NS300 equipped with Nanosight Tracking Analyses Analytical Software (Malvern Panalytical Ltd, Malvern, United Kingdom). The number of ASC-EVs released per cell was calculated as reported in the online Data Supplement.

Guava FACS Analysis

The characterization of EV surface molecules was performed by GUAVA FACS (fluorescence-activated cell sorting) analysis (GUAVA EasyCyte 8, Millipore) using MACSPlex exosome kit (Miltenyi biotech). Briefly, ASC-EVs were incubated with the antibody-coated capture Beads and subsequently ASC-EVs, bound to the MACSPlex Exosome Capture Beads, were labeled with the MACSPlex Exosome Detection Reagents containing different antibodies recognizing different surface markers. Control antibodies were also used. Consequently, the sandwich complexes formed among the MACSPlex Exosome Capture Bead, ASC-EVs, and the detection reagent were analyzed based on the fluorescence generated by the MACSPlex Exosome Capture Bead and the detection reagents. ASC-EVs fluorescence mean intensity was analyzed for each antibody and compared with the controls following manufacturer's instruction.

Transmission Electron Microscopy

Purified EV samples were analyzed as previously described placed on 200 mesh nickel formvar carbon-coated grids (Electron Microscopy Science, Hatfield, Pennsylvania) and left to adhere for 20 minutes. Next, grids were incubated with 2.5% glutaraldehyde containing 2% sucrose for 10 minutes and extensively washed in distilled water. Samples were than negatively stained with NanoVan (Nanoprobes, Yaphank, NY) and analyzed using a Jeol JEM 1010 electron microscope (Jeol, Tokyo, Japan).[17]

NRG1 ELISA Assay

ELISA assay was performed on protein derived from different ASC-EV preparations. Briefly, 100 µL of ASC-EV proteins were loaded in a microtiter plate provided by NRG1 ELISA kit (mybiosource) that has been coated with an anti-NRG1 specific antibody. Details are reported in the online Data Supplement.

Molecular Characterization of ASC-EV Cargo

ASC-EV proteins from different preparations (n=8) were extracted using a lysis buffer provided by the Human L1000 (Glass Slide) protein array kit (Ray biotech). This kit allows the detection of 1000 different proteins, including cytokines, chemokines, adipokines, growth factors, angiogenic

factors, proteases, soluble receptors, adhesion molecules, and other proteins to be simultaneously investigated.

Approximately 25 µg of protein were loaded for each sample. The fluorescence signal was subjected to background subtraction, and the cutoff threshold was set as >150 fluorescence intensity AU.

A PCR (polymerase chain reaction) angiogenesis array was performed on total RNA that had been extracted from ASC-EVs (n=7) using a miRVANA isolation kit and quantified using a NanoDrop1000 spectrophotometer. The RT^2 First Strand kit (SABiosciences) was employed for cDNA synthesis, according to manufacturer's instructions. Two hundred nanogram of cDNA was run on an Angiogenesis RT^2 Profiler PCR Array (PAHS 024, Qiagen, Frederick, MD) to profile 84 key genes involved in angiogenesis (list of genes available on website: https://www.thermofisher.com).

Data from the protein and mRNA arrays were compared, and pathway enrichment analysis was performed using Funrich 3.1.3.[18] Data were considered significant at $P<0.05$ (Hypergeometric test with Bonferroni correction). Interaction network on selected proteins/genes was built using STRING (protein-protein interaction network functional enrichment analysis) online software. Details are reported in the online Data Supplement.

Cell Culture

C2C12 cells (C2C12) were purchased from ATCC (American type culture collection) and cultured in Dulbecco's modified eagle medium (DMEM) high glucose (4.5 g/L-Lonza, Basel, Switzerland) and 20% FBS (Lonza). HMEC-1 (human microvascular endothelial cells-1) were purchased from ATCC and cultured in Endothelial basal medium (Lonza) and 10% FBS. SCs were isolated from the gastrocnemius muscles of C57BL/6J wild type mice subjected to ischemia. To obtain SCs, muscle samples were subjected to enzymatic digestion, as previously described.[15]

In Vitro Assays

In vitro hypoxia model. The following in vitro model was used to simulate I/R injury in vitro: cells (C2C12, differentiated myoblasts or HMECs) were cultured in a hypoxic gas mixture (1% O_2) for 8 hours in normal culture medium both with and without FBS. After hypoxia, cells were cultured in normoxic conditions, both with and without ASC-EVs (10 000 EVs/target cell), for 16 hours and then analyzed for proliferation, apoptosis, RNA and protein expression for 6 days, for the differentiation experiments as described below.

Myoblast differentiation into myotubes: C2C12 were cultured in DMEM high glucose (4.5 g/L-Lonza, Basel, Switzerland) and 20% FBS (Lonza). When cells reached 80% confluence, cells were cultured in high glucose plus 2% horse serum DMEM for 6 days. In selected experiments, C2C12 were cultured in hypoxic gas mixture (1% O_2) for 8 hours and then cultured in normoxic conditions, both with and without 2% horse serum and ASC-EVs, for 6 days.

Proliferation, C2C12 and HMEC proliferation was performed via 5-bromo-2-deoxyuridine (BrdU; Roche Diagnostics, Mannheim, Germany) incorporation in cells cultured in hypoxic conditions and incubated both with and without ASC-EVs. Details are reported in the online Data Supplement.

Apoptosis analysis in myoblasts and myotubes: C2C12 apoptosis was analyzed using MUSE CELL Analyzer (Millipore), and a double-staining with Annexin V and 7AAD. Briefly, cells were plated in 6 well plates, cultured in hypoxic gas mixture (1% O_2) for 8 hours and then cultured in normoxic conditions, both with and without ASC-EVs, for 16 hours and then analyzed. Myotube

apoptosis was evaluated by counting the fragmented nuclei stained with Hoechst staining. Briefly, differentiated C2C12, plated in 6 well plates, were cultured in hypoxic gas mixture (1% O_2) for 8 hours and then cultured in normoxic conditions, both with and without ASC-EVs, for 16 hours. Normal and fragmented nuclei were counted in microphotographs that were obtained using a fluorescence microscope, and the percentage of apoptotic cells was calculate as the ratio between the number of fragmented nuclei and the number of total nuclei per microscopic field. In selected experiments, ASC-EVs pretreated with a blocking NRG1 antibody, trypsin (0.25% w/v) and rhNRG1 (45 pg equivalent to 1.5×10^9 ASC-EVs/1.5×10^5 cells) were used. Details are reported in the online Data Supplement.

RT-PCR Array Analysis

The Skeletal Muscle Myogenesis and Myopathy RT^2 Profiler PCR Array (PAMM-099Z, Qiagen) was used to characterize the gene expression profiles of the healthy and ischemic gastrocnemius muscles of C57BL/6J, both those treated with ASC-EVs and those untreated.

Briefly, according to manufacturer's instructions, RNA extracted from mouse muscles using the miRVANA kit was treated with gDNA elimination buffer to degrade DNA contamination, and then reverse-transcripted using RT^2 First Strand kit. Data analysis was performed using the RT2 Profiler PCR Array Data Analysis tool provided by the manufacturer (thermofischer). The expression levels of each gene were normalized for housekeeping genes, according to manufacturer's instructions. Details are reported in the online Data Supplement.

Real-Time PCR Analysis

The total RNA from the ischemic gastrocnemius muscles of C57BL/6J and hypoxic C2C12 (both those treated with ASC-EVs and those untreated) were analyzed. Different primers for mouse MyoD, Myogenin, Myf5, Pax7 (paired box protein 7), p21, and p27 (Table I in the online-only Data Supplement) were used. Data analysis was performed using ExpressionSuite software (Life Technologies). In selected experiments, the EGR1 (early growth response 1) gene was evaluated. The primer sequences are reported in Table I in the online-only Data Supplement. Details are reported in the online-only Data Supplement.

Western Blot

ASC-EVs, C2C12, and SCs were lysed in lysis buffer (RIPA buffer with proteinase inhibitors, Sigma Aldrich) for 1 hour at 4°C and centrifuged at 10 000 rcf. The supernatants were collected, quantified using the Bradford method, and analyzed by Western blot. The following primary antibodies were used: NRG1 (Raybiotech), CD63, MyoD, myogenin, CdK6, pho-p38MAPK, p38MAPK (P38 mitogen-activated protein kinase), Cyclin D1, p-Bcl-2, Bcl-XL, β-actin, and vinculin (Santa Cruz). Densitrometric analysis was performed by Image Lab Software (BioRad), and data were expressed as arbitrary unit±SD. Details are reported in the online-only Data Supplement.

Statistical Analysis

Between-group comparisons were performed by *t* test. Our data passed normality and equal variance tests. Comparisons between 3 or more groups were performed by one-way ANOVA, and significance was evaluated using the Newman-Keuls multi-comparison *post hoc* test. The cutoff for statistical significance was set at $P<0.05$. All statistical analyses were performed on Graph Pad Prism version 5.04 (Graph Pad Software, Inc).

RESULTS

Characterization of ASC-EVs

ASC-EVs were analyzed for their surface markers using Guava FACS analysis (Figure I in the online-only Data Supplement). ASC-EV modal particle size corresponds to 160 nm (Figure IA in the online-only Data Supplement). No significant differences in ASC-EV number and size were observed over the various batches by Nanosight analyses. ASCs produced 11 411±2316 EVs per cell, after overnight starvation. Detailed information to estimate EV number is reported in the online-only Data Supplement. Starting from 2.25×10^{11} of total particles, the recovery of RNA and protein was similar in all the samples analyzed (n=21); about 275±31 ng of RNA and about 30.52±2.27 µg of protein. CD63, CD81, and CD9 exosomal marker expression was also detected using the MACSPlex kit for GUAVA FACS analysis (Figure IB in the online-only Data Supplement). Moreover, ASC-EVs showed the expression of CD29, CD44, and CD105 (ASC markers) and HLA I (Figure IB in the online-only Data Supplement). TEM was also performed and reported in Figure IC in the online-only Data Supplement.

ASC-EVs Prevent Muscle Damage in a Mouse Model of Hindlimb Ischemia

Preliminary experiments to identify the best administration route were performed by comparing 2 different administration routes as indicated in Materials and Methods section. Route 1: 1×10^{10} administrated intravenously immediately after intervention (T0), 0.5×10^{10} via intramuscular administration on day 1 (T1), and again on day 2 (T2); route 2: EVs were administered intramuscularly with the same timing and doses (T0:1×10^{10}; T1:0.5×10^{10}; T2:0.5×10^{10}; Figure II in the online-only Data Supplement). Therefore, to evaluate ASC-EV protection, mice that were subjected to the acute ischemic hindlimb process were treated with 2×10^{10} ASC-EVs using the best administration route which corresponded to the route 1. The same volume of saline served as control. Blood perfusion of the ischemic hindlimb analyzed immediately after surgery by Laser Doppler, showed a strong reduction in blood flow (0.13±0.07 control group; 0.09±0.03 in ASC-EV group; Figure III in the online-only Data Supplement). Although, no significant differences in large vessel reperfusion were found in the treatment groups, the saline group showed significantly higher functional damage scores than the ASC-EV-treated group (Figure 1A). To evaluate whether functional differences were a result of improvement in tissue reperfusion, vessel number was tallied in the ischemic muscles of treated animals at different time intervals (day 3 and 7); ASC-EV-treated animals showed a higher number of vessels than the saline group on day 7 quantified as number of small capillaries per number of muscle fiber (Figure 1B and 1D and Figure IV in the online-only Data Supplement). No differences were obtained counting large vessels (not shown). Furthermore, an analysis of gastrocnemius muscles revealed the presence of focal areas of damage in the saline group. This effect was almost completely prevented by ASC-EV treatment (Figure 1C and 1D). These results suggest that, in our model, ASC-EV treatment protects muscles against ischemia-induced damage.

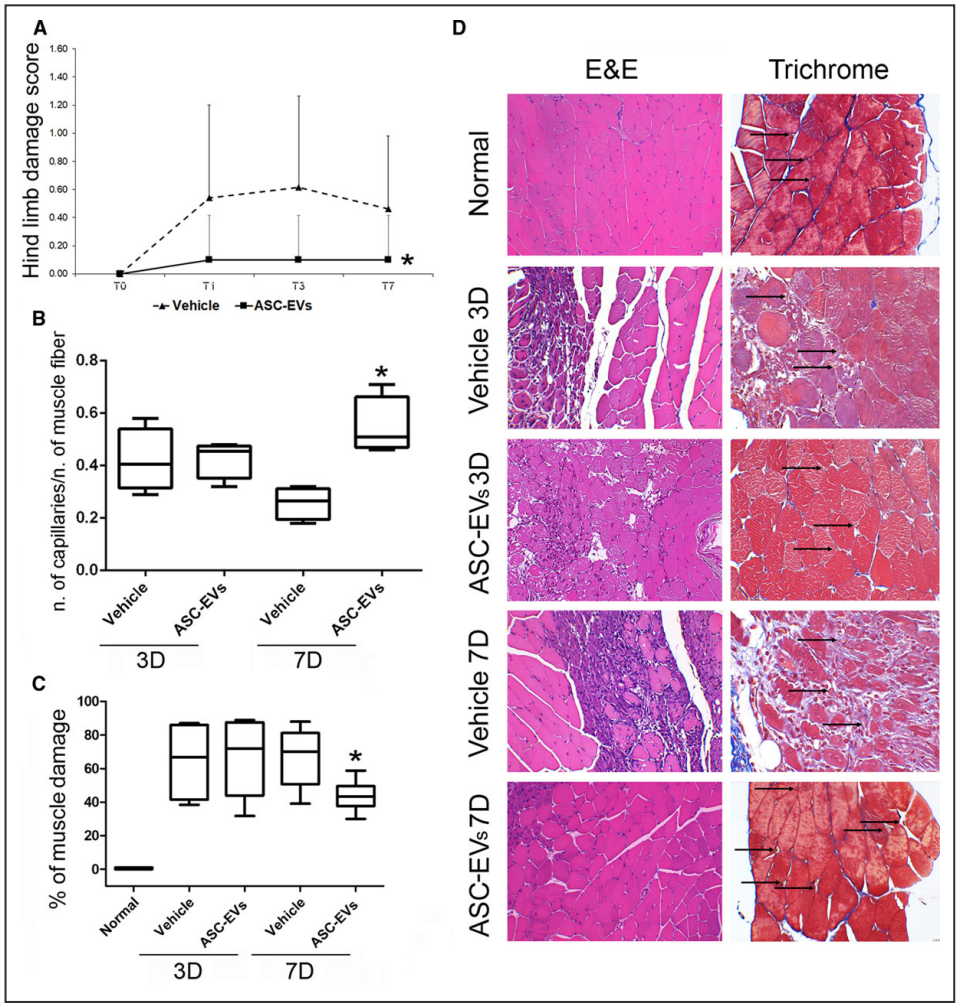

Figure 1. Effects of adipose stem cell-derived extracellular vesicles (ASC-EVs) on ischemia/reperfusion damage. A, Foot damage score on different days (0, 1, 3, 7) after surgery in ASC-EV treated and untreated mice. Data are expressed as mean±SD; **P* value<0.05 ASC-EVs vs Vehicle, (One-way Anova—Newman-Keuls Multiple Comparison Test), (n=8). **B**, Quantitative analysis of the capillary density of normal and ischemic hind limbs on days 3 and 7 after surgery. Data are expressed as mean±SEM number of capillaries/number of muscle fiber; **P* value <0.05, ASC-EVs vs Vehicle, (One-Way Anova—Newman-Keuls Multiple Comparison Test; n=8). **C**, Quantitative analysis of muscle damage areas in hematoxylin-eosin stained gastrocnemius muscles of normal and ischemic hind limbs on days 3 and 7 after surgery. Data are expressed as percentage of damage area±SEM; **P* value <0.05 ASC-EVs vs Vehicle, (One-way Anova—Newman-Keuls Multiple Comparison Test; n=8). **D**, Representative hematoxylin-eosin and Masson's trichrome images of nonischemic (normal) and ischemic hindlimb gastrocnemius muscles in Vehicle- and ASC-EV-treated animals after 3 (3D) and 7 (7D) days post-surgery (original magnification, ×200 for hematoxylin-eosin–scale bar: 50 μm and ×400–scale bar: 25 μm for Masson's trichrome). Arrows indicate the capillaries.

Gene Array Analysis of Muscles From ASC-EV-Treated Animals

To investigate the ASC-EV mechanism of action muscles recovered on day 3 after surgery were analyzed using a skeletal muscle-specific gene array. As shown in Table 1/Table I in the online-only Data Supplement and Figure 2A, ASC-EV treatment induced the expression of genes, such as MyoD, Myf5, and Pax7, that are involved in muscle cell proliferation, regeneration, and differentiation. Primary SCs, recovered from healthy muscles, were also subjected to in vitro I/R and treated or not with ASC-EVs to further validate these data. As shown in Figure 2B, the ASC-EVs induced the expression of MyoD. As expected, myogenin did not change on ASC-EV treatment (Figure 2A and 2B)

Table 1. List of mRNAs Modulated in ASC-EV-Treated Muscles, Compared With Untreated Muscles (Table view)

Gene Symbol	Fold Regulation	SD
Myod1	3.85	±0.30
Myf5	2.97	±0.18
IL6	2.89	±0.17
Cav1	2.33	±0.50
Igf2	2.03	±0.79
Ppargc1a	1.71	±0.59
Ppargc1b	1.71	±0.78
Igf1	1.69	±0.49
Ctnnb1	1.69	±0.67
Capn2	1.62	±0.31
Capn3	1.62	±0.51
Prkaa1	1.61	±0.58
Lmna	1.58	±0.24
Cs	1.57	±0.81
IL1b	1.55	±0.30
Agrn	1.55	±0.61
Mapk14	1.53	±0.75
Prkag1	1.52	±0.80
Pax7	1.52	±0.62
Ikbkb	0.65	±0.21
Foxo1	0.59	±0.15
Myh1	0.56	±0.18
Tgfb1	0.54	±0.25
Lep	0.24	±0.19

RQ (fold regulation) values are evaluated using: $2^{-\Delta\Delta Ct}$±SD (n=4). ASC-EV indicates adipose stem cell-derived extracellular vesicles.

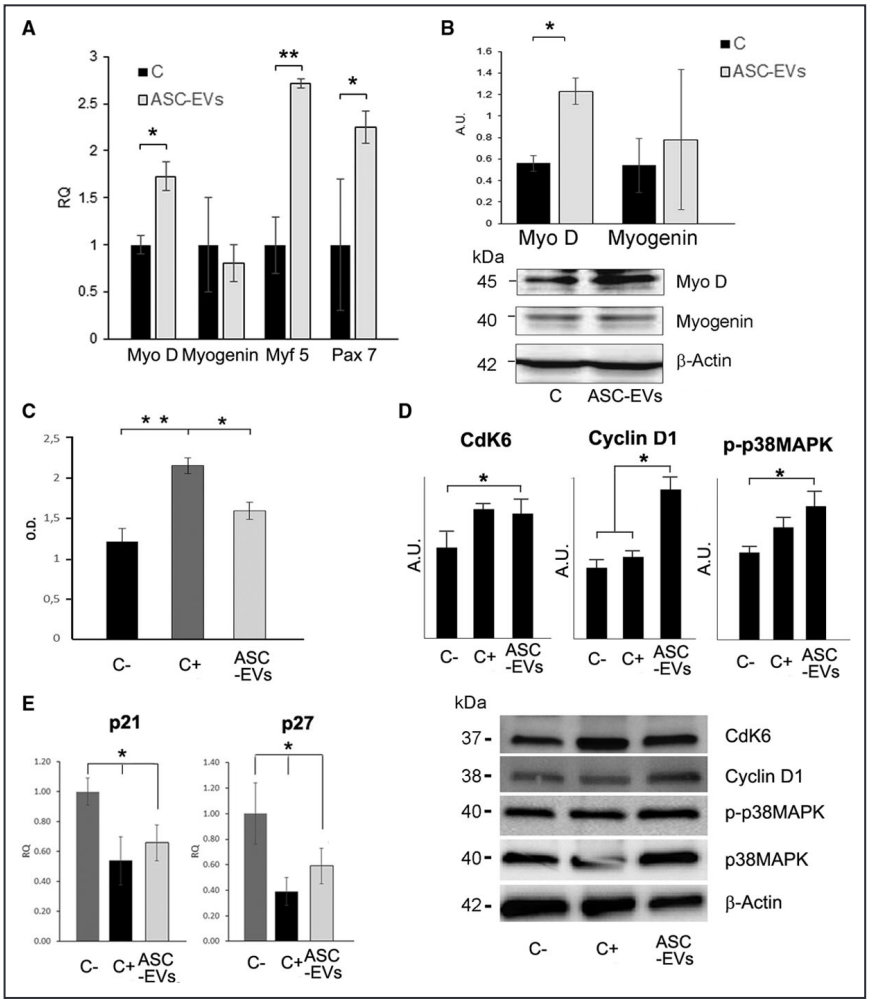

Figure 2. Adipose stem cell-derived extracellular vesicles (ASC-EVs) induce the expression of differentiation genes in muscles and in satellite cells exposed to ischemia/reperfusion (I/R) and induce proliferation on myoblast in vitro. A, Total RNA from I/R gastrocnemius muscles, both treated (ASC-EVs) and untreated (C) were analyzed for the expression of muscle differentiation genes (MyoD, Myogenin, Myf5, Pax7) by RT-PCR. Results are expressed as relative quantification (RQ) of data normalized for housekeeping genes. The results are representative of 3 different experiments (n=3; **P*<0.05 ASC-EVs vs C for MyoD, Pax7; ***P*<0.01 ASC-EVs vs C for Myf5). **B**, Satellite cells recovered from normo-perfused muscles were subjected to I/R. Cell extracts were analyzed for MyoD and Myogenin content by densitometry (Relative amount). Protein levels were normalized to β-actin content. The results are representative of 3 different experiments (n=3; **P*<0.05 ASC-EVs vs C). **C**, Myoblasts were cultured in hypoxic conditions in medium with (C+) or without (C−) FBS, in the presence and in the absence of ASC-EVs (ASC-EVs), and evaluated for BrdU incorporation (n=3; **P*<0.05 ASC-EVs vs C−; ***P*<0.01 C+ vs C−). **D**, Representative images and relative densitometric analysis of CdK6, Cyclin D1, and p-p38MAPK protein expression in myoblasts treated as above and normalized for either β-actin or p38MAPK. The same blot was used to evaluate CdK6, Cyclin D1, and p-p38MAPK expression. Results are representative of all samples (n=3; **P*<0.05 ASC-EVs vs C−). **E**, p21 and p27 RQ expression in myoblasts treated as above and normalized for the housekeeping gene (p21, p27: **P*<0.05 ASC-EVs vs C−).

ASC-EVs Induce Myoblast Proliferation

To validate the above data, the effect of ASC-EVs on myoblast proliferation was evaluated *using* murine myoblasts subjected to in vitro I/R. Based on our preliminary experiments using a variety of ASC-EV doses (data not shown), we decided to use 10000 EVs/target cell to evaluate ASC-EV biological effects. Fetal bovine serum treatment served as a positive control throughout the study. The proliferative effect of ASC-EVs on myoblasts that were subjected to treatment was evaluated. As shown in Figure 2C, ASC-EVs were able to induce myoblast proliferation in hypoxic conditions. Accordingly, cyclin D1 and CDK6 increased in myoblasts challenged with ASC-EVs (Figure 2D). The fact that myoblasts enter the cell cycle is also supported by p38/MAPK activation (Figure 2D).

These results were further validated by an analysis of the expression of cyclin kinase inhibitory genes, p21 and p27 (Figure 2E).

ASC-EVs Induce Myoblast Differentiation and Prevent Apoptosis of Both Myoblasts and Their Differentiated Counterparts

The effect of ASC-EVs on myoblast differentiation was also evaluated in vitro in murine myoblasts subjected to I/R. Data reported in Figure 3A, demonstrate that ASC-EV-treated myoblasts displayed a higher fusion index than untreated myoblasts. Moreover, the possibility that ASC-EVs may prevent apoptosis was also investigated. A double-staining, using annexin V and 7AAD, was performed. As shown in Figure 3B, ASC-EVs were able to increase the number of living cells and to reduce the number of apoptotic myoblasts. The expression of Bcl-XL and the phosphorylation of Bcl-2 were analyzed for validation purposes. As reported in Figure 3C, ASC-EV treatment was associated with the increased expression of Bcl-XL and the phosphorylation of Bcl-2.[19] The anti-apoptotic effect of ASC-EVs was also evaluated in differentiated myoblasts by analyzing the morphological alterations that occur in nuclei in the final stages of apoptosis. Data reported in Figure 3D indicate that ASC-EV treatment decreased the percentage of fragmented nuclei in differentiated myoblasts. Unlike proliferation (proliferating cell-nuclear antigen; Figure V in the online-only Data Supplement), that occurs rapidly after I/R damage, we were able to demonstrate the anti-apoptotic effects of ASC-EVs in vivo (Figure 3E). These data indicate that ASC-EVs can protect muscles from I/R-induced damage by inducing myoblast proliferation, differentiation and by preventing apoptosis.

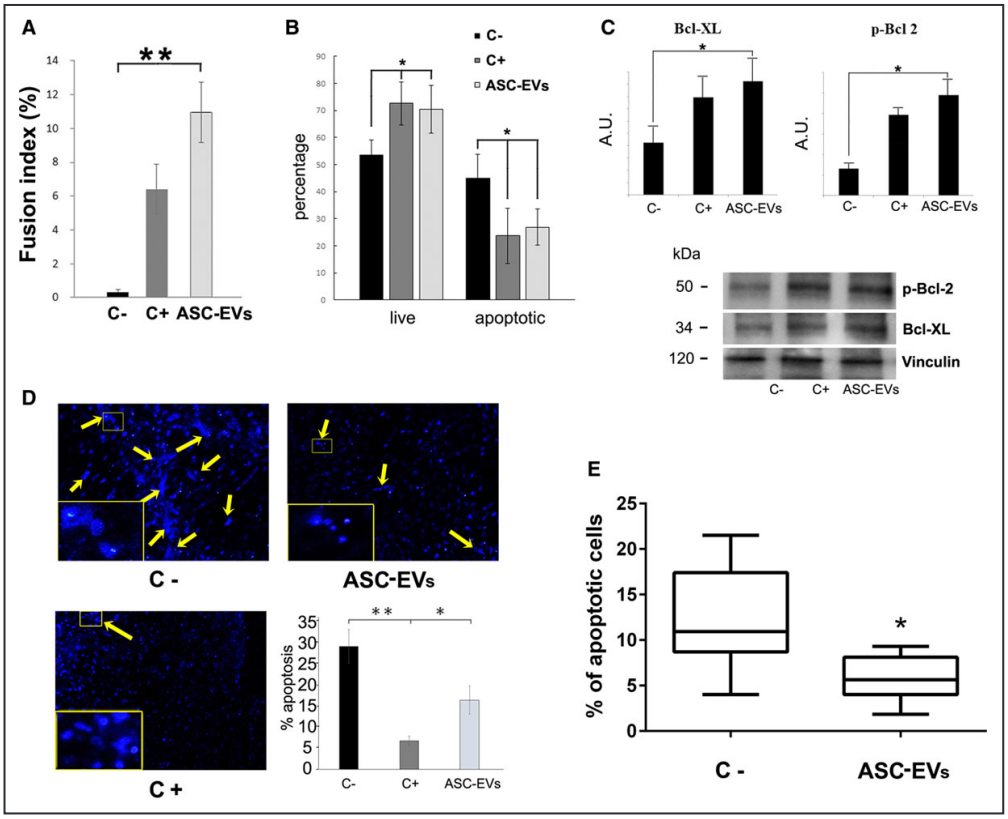

Figure 3. Effects of adipose stem cell-derived extracellular vesicles (ASC-EVs) on myoblast differentiation and apoptosis. A, After hypoxia, myoblasts were cultured in normoxic conditions in medium supplemented with 10% FBS (C−) either with 2% horse serum (differentiation condition) with ASC-EVs (ASC-EVs) or without ASC-EVs (C+; *P<0.05 ASC-EVs vs C−). Fusion index was calculated by the ratio between the number nuclei detected in myotubes expressing the myosin heavy chain (nuclei >2 was considered positive) and the total number of nuclei. **B**, Apoptosis assay on myoblasts cultured in hypoxic conditions in medium with (C+) or without (C−) FBS either in the presence (ASC-EVs) or absence of ASC-EVs (*P<0.05

C+ and ASC-EVs vs C−). **C**, Representative images and relative densitometric analysis of p-Bcl-2 and Bcl-XL protein expression in myoblasts treated as above and normalized for vinculin. The same blot was used to evaluate p-Bcl-2 and Bcl-XL protein expression. Results are representative of all samples (n=5; **P*<0.05 ASC-EVs vs C−). **D**, Representative images and quantification of nuclei fragmentation in myotubes cultured in hypoxic conditions in the presence (C+) and the absence (C−) of FBS, both with and without ASC-EVs (n=3; **P*<0.05 ASC-EVs vs C−, ***P*<0.01 C+vs C−; yellow arrows indicate apoptotic nuclei). **E**, Apoptosis in ischemic muscles was evaluated at day 7 after surgery upon ASC-EV (ASC-EVs) or saline treatment (C−). The expression of the percentage of apoptotic cells is reported (**P*<0.05 ASC-EVs vs C−).

ASC-EV Cargo Drives Pro-Angiogenic and Skeletal Muscle Protection Mainly Via NRG1-Mediated Signals

ASC-EVs were analyzed for their protein content. In particular, a protein array slide for the detection of cytokines, chemokines, adipokines, growth factors, angiogenic factors, proteases, soluble receptors, and soluble adhesion molecules was used. As shown in in the online-only Data Supplement Table II, 237 proteins were detected in ASC-EVs. The most abundant proteins are reported in Table 2.

Table 2. List the Most Abundant Proteins in ASC-EVs (Table view)

Protein	Gene Name	Fluorescence Intensity	SD
Neuregulin 1	NRG1	50176	±10353.11
LAG-3	LAG3	1979	±184.91
Amylin	IAPP	753	±144.60
IL-21	IL21	647	±88.75
IL-13	IL13	632	±80.76
GDF11	GDF11	626	±129.04
HGFR	MET	625	±123.97
MSHa	MSX1	590	±43.49
GDF3	GDF3	587	±78.70
Granzyme A	GZMA	573	±13.92
BD-1	DEFB1	563	±54.33
GDF5	GDF5	556	±73.55
GDF9	GDF9	552	±80.80
MIP-3 beta	CCL19	539	±153.82
GRO	CXCL2	533	±21.26
IFN-gamma	IFNG	530	±34.57
GDF8	MSTN	527	±51.67
IL-5	IL5	512	±27.15

ASC-EV indicates adipose stem cell-derived extracellular vesicles.

It is interesting to note that ASC-EVs were found to be enriched in NRG1 (Table 2, Figure 4A). ELISA assay demonstrated that 1×10^{10} ASC-EVs contain 300±7.07 pg of NRG1. NRG1 acts by binding to the ERBB tyrosine kinase receptors which activate a cascade of signaling pathways, including the p38MAPK pathway.[20] NRG1 controls both the proliferative and myogenic processes in skeletal muscle cells,[21] while it drives endothelial cell proliferation in response to ischemia.[22] A blocking antibody against NRG1 was used to evaluate NRG1's contribution to ASC-EV-mediated protection. To this end, the BrdU assay and the expression of p38MAPK, cyclin D1 or p-Bcl-2 and

Bcl-XL were evaluated in myoblasts subjected to ASC-EV treatment. As shown in Figure 4B through 4D, the NRG1 blockade prevented ASC-EV-mediated myoblast proliferation and the transcription of EGR1, the NRG1 early response gene,[23] while it was ineffective in preventing protection against I/R induced apoptosis (Figure 4E). rhNRG1 served as positive internal control. Moreover, the effect of the NRG1 blockade was also evaluated in endothelial cells subjected to ischemia as the involvement of NRG1 in endothelial cell proliferation has already been reported.[24] The results described in Figure 4F clearly demonstrate that ASC-EV-mediated endothelial cell proliferation and EGR1 transcription (Figure VI in the online-only Data Supplement) were inhibited by the NGR1 blockade. Finally, the pretreatment of ASC-EVs with trypsin demonstrates that ASC-EV-mediated biological effects rely on having NRG1 bound to their membrane (Figure 4C and 4F).

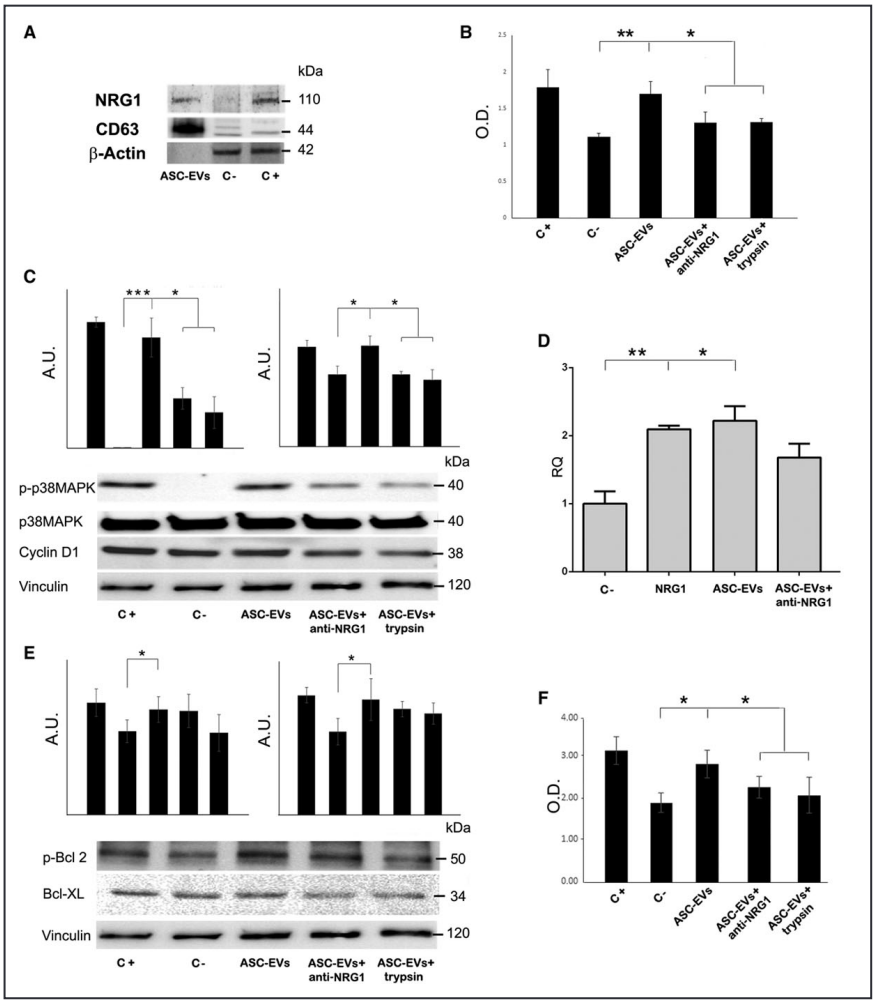

Figure 4. Role of NRG1 (neuregulin 1) in adipose stem cell-derived extracellular vesicles (ASC-EV)-mediated myoblast and endothelial cell proliferation. A, Expression of NRG1, CD63, and vinculin in ASC-EVs, renal tubular (C−), and myotube cells (C+) were used as negative control and positive control respectively.

B, BrdU (5-bromo-2-deoxyuridine) analysis of myoblasts cultured in hypoxic conditions, with (C+) and without (C−) FBS, in the presence and in the absence of ASC-EVs (ASC-EVs), ASC-EVs treated with an anti-NRG1 blocking antibody (ASC-EVs+anti-NRG1) or with trypsin (ASC-EVs+trypsin; n=3; ***P*<0.01 ASC-EVs vs C−; **P*<0.05 ASC-EVs vs ASC-EVs+anti-NRG1 and ASC-EVs+trypsin). **C** and **E**, Myoblasts cultured as above and evaluated for p-p38MAPK, Cyclin D1 (**C**), p-Bcl-2 and Bcl-XL (**E**). The same blot was used to evaluate p-p38MAPK, Cyclin D1, p-Bcl-2, and Bcl-XL protein expression. Densitometric analysis of C and E (Relative amount). Protein levels were normalized to p38/MAPK and vinculin. (n=3; **P*<0.05 ****P*<0.001). **D**, Quantitative real-time polymerase chain reaction analysis of ERG1 in myoblasts cultured in hypoxic condition for 1 hour, without FBS (C−), with rhNRG1, ASC-EVs (ASC-EVs) or ASC-EVs treated with an anti-NRG1 blocking antibody (ASC-EVs+anti-NRG1; n=3; **P*<0.05 C− vs NRG1, ***P*<0.01 C− vs ASC-EVs) is reported. **F**, BrdU incorporation in human endothelial cells (HMECs) cultured in hypoxic conditions in medium, with (C+) and without (C−) FBS, in the presence and in the absence of ASC-EVs (ASC-EVs), ASC-EVs treated

with an anti-NRG1 blocking antibody (ASC-EVs+anti-NRG1) and with trypsin (ASC-EVs+trypsin; n=3 *P<0.05 ASC-EVs vs C−; *P<0.05 ASC-EVs vs ASC-EVs+anti-NRG1 and ASC-EVs+trypsin).

NRG1 Blockade Prevent ASC-EV Action In Vivo

To further validate the above data, ASC-EVs pretreated with the anti-NRG1 blocking antibody were used for the in vivo study. As shown in Figure 5A through 5C the NRG1 blockade abrogates the ASC-EV pro-angiogenic effects as well as their protection against muscle damage (Figure 5B and 5C). Moreover, muscle damage was also evaluated at day 7 using nitro-blue tetrazolium-staining. As shown in Figure 5B and Figure VII in the online-only Data Supplement, ASC-EV were able to significantly reduce the ischemic area, while NRG1 blockade completely abrogated their effect. Of note, we failed to detect muscle protection when rhNRG1 was used as purified factor (300 pg; data not shown). It has been recently shown that ASC-EV, obtained from patients undergoing abdominal surgery, promote inflammation in a preclinical model of I/R.[25] Our data clearly demonstrated that ASC-EV treatment did not increase the number of inflammatory cells (shown by CD14 staining) in the ischemic muscles (Figure 5A and 5C). Moreover, consistent with the potential role of NRG1 in regulating the inflammatory response,[26] we found that ASC-EVs pretreated with the anti-NRG1 blocking antibody were no more effective in preventing the recruitment of inflammatory cells (Figure 5A and 5C) and in promoting neoangionesis (Figure 5B and 5C and Figure VIII in the online-only Data Supplement).

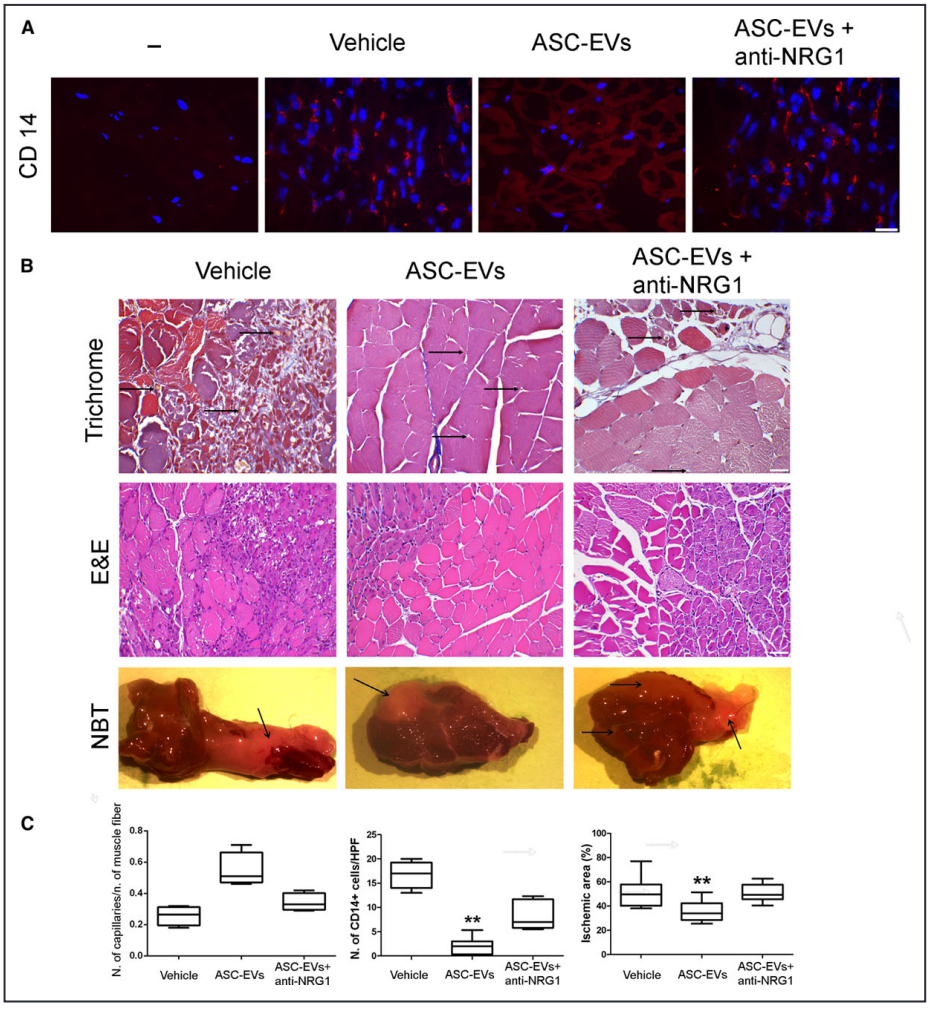

Figure 5. Adipose stem cell-derived extracellular vesicles (ASC-EVs) prevent the inflammatory response via NRG1 (neuregulin 1). A, Representative immunofluorescence images of inflammation. Anti-CD14 mAb was used to analyze gastrocnemius muscles of ischemic hindlimb in Vehicle, ASC-EVs- and ASC-EVs+anti-NRG1 treated animals as indicated (original magnification: ×400—scale bar: 25 μm). The

negative control for primary antibodies is indicated as "−".
B, Representative hematoxylin-eosin, and Masson's trichrome, and NTB images of gastrocnemius muscles of ischemic hindlimb in Vehicle, ASC-EVs and ASC-EVs+plus anti-NRG1 treated animals (original magnification: ×200 for hematoxylin-eosin–scale bar: 50 μm and ×400–scale bar: 25 μm for Masson's trichrome). Arrows indicate the capillaries and the ischemic area in the NTB sections. **C**, Quantitative analyses of capillaries (number of capillaries/number of muscle fiber), CD14+cells and the percentage of the ischemic area in Vehicle, ASC-EV and ASC-EV plus anti-NRG1 ischemic hindlimb at day 7 after surgery are reported. Data are expressed as mean±SEM; *P value <0.05, ASC-EVs vs Vehicle, (One-Way Anova - Newman-Keuls Multiple Comparison Test; n=8 for quantification capillary density and CD14+ cells, and n=4 for NTB analysis).

ASC-EV mRNA and Protein Cargo Can Co-Operate to Boost Angiogenesis and Muscle Regeneration After I/R Damage

To gain further insight into the ASC-EV mechanism of action, ASC-EV mRNA content was analyzed using an RT-PCR array for the detection of the genes involved in angiogenesis. It is worth noting that gene array analysis highlighted enrichments in fibronectin 1, MMP2 (matrix metallopeptidase 2), angiopoietin, FGF2 (basic fibroblast growth factor), VEGFA (vascular endothelial growth factor A), and FLT1 (Fms-related tyrosine kinase 1) mRNA. Moreover, the well-known modulators of both angiogenesis and muscle regeneration, HGF (hepatocyte growth factor), IGF1 (insulin-like growth factor-1), and EGF (epidermal growth factor) mRNA, were also found to be highly expressed (Table 3). A comparison of mRNA and the protein microarray led to 18 molecules being commonly detected in ASC-EVs (Figure 6A and 6B). Pathway enrichment analysis demonstrated that they are mainly involved in VEGF, sphingosine 1-phosphate, PDGF, EGF, HGF, and uPAR (urokinase-type plasminogen activator receptor) mediated signaling pathways (Figure 6C). Moreover, the interaction graph shown in Figure 6D indicates that there is close interplay between these molecules, which sustains the idea that they cooperate to induce angiogenesis and muscle regeneration in our model.

Table 3. Complete List of mRNAs Involved in Angiogenesis Analyzed in ASC-EVs (Table view)

Gene Symbol	40–Ct (± SD)	Gene symbol	40–Ct, (± SD)	Gene Symbol	40–Ct, (± SD)
FN1	9.57±0.79	ANGPT1	7.33±0.53	ANGPTL4	6.63±0.72
COL4A3	8.76±0.68	TIMP2	7.29±0.84	ANG	6.61±0.49
PGF	8.76±0.81	IL6	7.28±0.87	ENG	6.55±0.95
MMP2	8.49±0.71	TIMP1	7.24±2.1	PTGS1	6.49±1.34
PLG	8.31±0.68	SERPINF1	7.24±1.11	CCL2	6.47±0.54
HGF	8.31±0.79	AKT1	7.21±0.99	VEGFC	6.43±1.11
IGF1	8.30±0.71	ANPEP	7.21±0.76	EFNA1	6.37±0.91
TEK	8.24±0.75	EFNB2	7.20±0.51	TNF	6.29±0.66
FGF2	8.19±0.66	CXCL6	7.19±0.85	CTGF	6.29±0.50
HIF1A	7.98±0.59	HPSE	7.09±0.86	NOS3	6.13±0.84
VEGFA	7.94±0.73	THBS1	7.07±1.10	VEGFB	6.12±0.79
EDN1	7.93±1.34	EPHB4	7.05±0.57	CXCL5	6.10±0.55
PF4	7.85±0.64	NRP1	7.03±0.81	LECT1	6.08±1.08
CXCL9	7.78±0.69	THBS2	7.02±0.87	CDH5	5.97±0.74
FGF1	7.77±0.82	CCL11	7.01±0.91	LEP	5.92±0.73
TGFB2	7.73±0.61	TGFA	6.94±0.58	ITGB3	5.85±0.91
ITGAV	7.71±0.79	TIE1	6.92±0.83	MMP14	5.78±0.71
PROK2	7.69±0.93	TGFB1	6.89±0.72	IL1B	5.72±0.76

Gene Symbol	40–Ct (± SD)	Gene symbol	40–Ct, (± SD)	Gene Symbol	40–Ct, (± SD)
EGF	7.6±0.98	COL18A1	6.89±0.61	SPHK1	5.57±0.75
FLT1	7.57±0.64	PDGFA	6.85±0.59	PLAU	5.48±0.73
IL8	7.55±0.78	KDR	6.84±0.38	FGFR3	5.38±0.79
IFNG	7.51±0.88	F3	6.83±0.57	ID1	5.14±0.81
IFNA1	7.50±0.67	TGFBR1	6.81±1.19	S1PR1	5.08±0.83
SERPINE1	7.46±0.75	BAI1	6.79±0.70	ERBB2	5.03±0.63
FIGF	7.45±0.50	NRP2	6.78±0.61	PECAM1	4.91±0.46
TIMP3	7.42±0.72	ANGPT2	6.75±0.48	NOTCH4	4.80±0.97
JAG1	7.39±0.92	MMP9	6.71±0.75	TYMP	4.51±0.61
CXCL10	7.38±1.06	CXCL1	6.68±0.71	MDK	3.27±0.65

40–Ct values were calculated by subtracting the mean gene Ct from 40 total real-time polymerase chain reaction cycles (±SD).

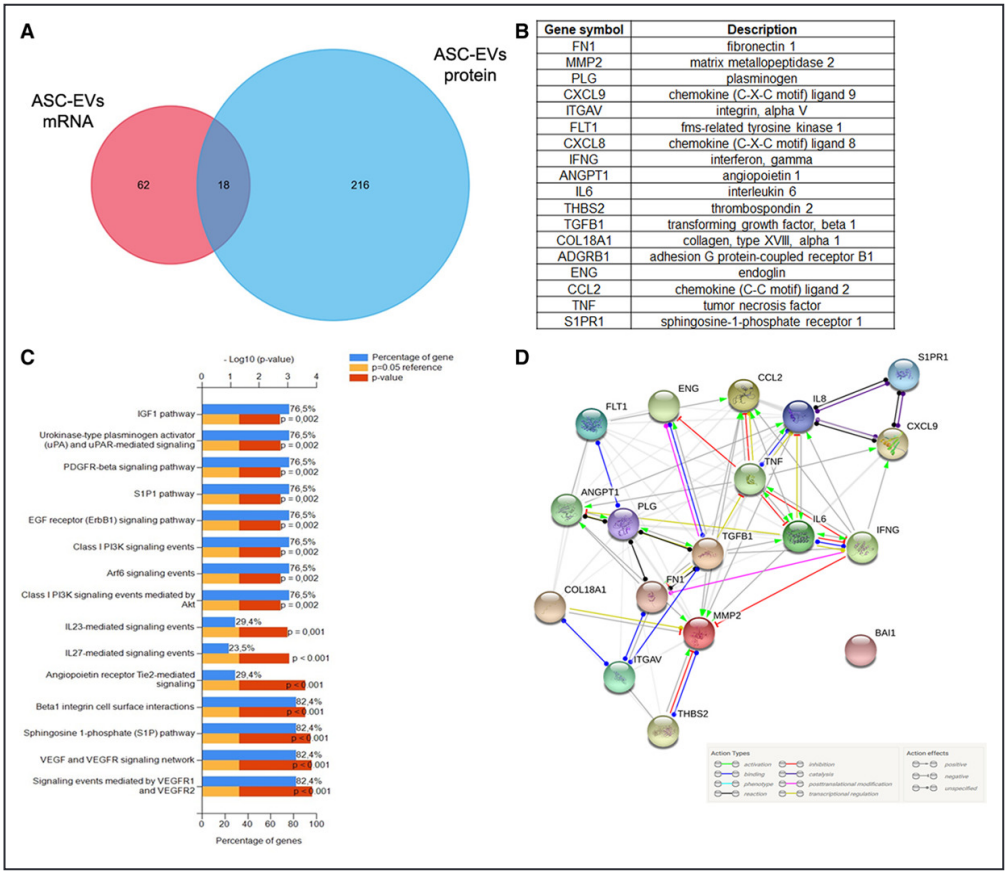

Figure 6. **Adipose stem cell-derived extracellular vesicles (ASC-EV) cargo characterization and pathway enrichment analysis. A**, Venn diagram showing the comparison between mRNAs and proteins carried by ASC-EVs.

B, List of the 18 molecules carried by ASC-EVs, such as mRNAs and proteins. **C**, Biological pathways in which the 18 mRNA/proteins are mainly involved. Many enriched pathways are related to angiogenesis and muscle regeneration. Bioinformatic analysis was performed using Funrich V3 software. The blue bar represents the percentage of genes involved in the specific pathway; the red bar represents the significant *P* value ($P<0.05$ Hypergeometric test with Bonferroni test correction). **D**, Interaction graph analyzed by String on line software showing relationship between the 18 identified proteins. Red arrows indicate inhibition; green arrows indicate activation; blue arrows indicate protein binding.

DISCUSSION

Critical limb ischemia is a common feature of patients with peripheral artery disease.[1,27] Since current therapeutic options are still ineffective new therapeutic strategies with which to improve patient outcomes are required. Adult stem cells are emerging as a cell-based therapy.[4] Of the stem cells available, ASCs are an ideal source.[5] They are easy available, show low immunogenicity and high proliferative capability[5] and were found effective in preclinical models of muscle atrophy[28] and peripheral artery disease.[29]

A number of evidence indicates that advantages may be provided by secretome derivatives of stem cells, including EVs,[5] in regenerative medicine and in therapeutic angiogenesis.[30] Herein, we investigated whether ASC-EVs could become a therapeutic tool with which to improve angiogenesis in mice that recapitulate human critical limb ischemia. We have demonstrated that ASC-EVs display pro-angiogenic effects in vivo, as shown by the number of capillary/muscle fiber and by the analysis of capillary density. We have also found that mice treated with ASC-EVs present a lower score for hindlimb functional damage than mice treated with the vehicle alone. Accordingly, histological analyses have highlighted that mice subjected to ASC-EV treatment had a reduced percentage of apoptotic cells and muscle damage. After damage, SCs enter the cell cycle by activating p38MAPK and inducing the expression of MyoD in the daughter cells.[11] Transcriptomic analysis, performed to detect early molecular events, has demonstrated that ASC-EV treatment induced the expression of genes associated with myoblast proliferation and differentiation, such as MyoD, Pax7, and Myf5, on day 3 after surgery. In accordance with these results, SCs that were exposed to ASC-EVs in ischemic/reoxygenation conditions increased the expression of MyoD. We further validated these data in vitro. Indeed, it has been demonstrated that ASC-EV challenge leads to an increase in the number of BrdU positive myoblasts. Accordingly, cyclin D1, CDK6, and p-p38/MAPK expression increased. Along with the effect on myoblast proliferation, we have also been able to demonstrate that ASC-EVs induced myoblast differentiation and prevented apoptotic signals in both myoblasts and their differentiated counterparts. As a matter of fact, ASC-EVs were able to increase the expression of Bcl-XL and the phosphorylation of Bcl2[19] in myoblasts and reduce the number of fragmented nuclei in differentiated myoblasts. These results sustain the possibility that protection against apoptosis and induction of vessel formation may well be the most relevant mechanisms via which a fast muscle regeneration/protection occurs. In line with this hypothesis, we failed to detect an increased number of regenerating myofibers and a decreased number of apoptotic cells at day 7 in ASC-EV-treated animals.

mRNAs, miRNAs, proteins, and bioactive lipids are all recognized as relevant mediators of EV biological action in different regenerative processes.[7] However, miRNAs are the most studied pro-angiogenic drivers of stem-cell derived EV activities. This is also true for ASC-EVs.[31–33] We have demonstrated herein that ASC-EVs are also enriched in mRNAs that encode for a number of angiogenic regulators. More importantly, proteomic analyses of ASC-EV cargo has indicated relevant enrichment in NRG1, which is a member of the epidermal growth factor family that is also produced by skeletal muscles.[34,35] NRG1 regulates muscle cell homeostasis, SC survival and many relevant biological processes in skeletal muscles.[36] It exerts its biological effects by binding to NRG1 receptors, including ErbB3 and ErbB4 and the co-receptors ErbB1 and ErbB2.[35] We herein report that ASC-EV-delivered NRG1 may be involved in muscle protection against I/R damage, as is consistent with previous observations that demonstrate the involvement of the NRG1/ErbB system in muscle regeneration.[20] As a matter of fact, in vitro NRG1 blockade prevented the activation of p-p38MAPK, the expression of cyclin D1 and the transcription of ERG1 in myoblasts treated with ASC-EVs and subjected to I/R. These biochemical events in vitro

translated into the inhibition of myoblast proliferation and in vivo in the prevention of ASC-EV-mediated protection, as also supported by tetrazolium-staining. On the contrary, an NRG1-independent mechanism seems to be associated with protection against I/R-induced apoptosis in response to ASC-EV treatment. The IL-21R/IL-21 axis has been shown to prevent apoptosis and favor cell survival in hypoxic conditions.[37] Indeed, ASC-EVs were also enriched in IL-21, suggesting that ASC-EV-treatment-associated apoptosis resistance may rely on the IL-21-mediated signaling pathway. Further studies are required to validate this hypothesis.

It has been reported that endothelial cells express both NRG1 and its receptors,[24] and Hedhli et al[22] have more recently demonstrated that NRG1 of endothelial origin is a crucial mediator of both angiogenesis and arteriogenesis in a hindlimb ischemia model. In a finding that is consistent with these results, we have demonstrated that, just like in myoblasts, ASC-EVs promote endothelial cell proliferation and ERG1 transcription in hypoxic conditions and that these effects rely on ASC-EV-membrane-bound NRG1.

The recruitment of inflammatory cells is necessary to promote vascular growth on damage. However, it has been recently shown that ASC-EVs, obtained from patients undergoing abdominal surgery, increased the recruitment of inflammatory cells without protecting muscles against I/R damage.[25] Of note, improvement of blood perfusion, protection of muscles, and a reduced infiltration of inflammatory cells were observed in mice treated with ASC-EVs released in response to PDGF (platelet-derived growth factor).[25] The increase of IL-10 and TGF-β1 (transforming growth factor beta 1) secretion by the inflammatory cells has been suggested to play a role in PDGF-driven ASC-EV action. This suggests the possibility that immunomodulatory mechanisms may be activated by ASC-EVs, including those mediated by NRG1.[26] Nonetheless, possibly due to the enrichment of pro-angiogenic mediators, ASC-EVs could induce a compensatory vascular growth able to protect muscle from damage even in the presence of a reduced number of inflammatory cells.

The existence of a dual ASC-EV biological effect, made up of angiogenesis and a hasty muscle protection, is therefore sustained by our in vivo results. Moreover, pathway enrichment analysis and, more importantly, the interaction graph further support the notion that cooperation between the bioactive molecules carried by ASC-EVs sustain and boost biological effects in our preclinical I/R model. This co-operative activity may provide a further explanation as to NRG1's independent protection against apoptosis in myoblasts and their differentiated counterparts, as well as to the failure of 300 pg rhNRG1, corresponding to its ASC-EV content, to recapitulate ASC-EV therapeutic effects.

EV therapeutic approaches have been proposed to solve a number of concerns about stem cell-based therapy in a range of clinical settings.[5] Our data demonstrate that the off-the-shelf ASC secretome may be a useful therapeutic approach with which to improve vascular growth and to protect muscles from I/R-mediated damage. Moreover, we have also identified NRG1 as one of the most relevant mechanisms for ASC-EV biological activity. Effort should now be placed into investigations of the therapeutic potential that ASC-EVs show for the treatment of a variety of pathological conditions in which muscle protection is required.

Limitations

We are confident that the intrinsic curb of Laser Doppler Perfusion analysis, prevents the detection of the profound vascular districts. However, histological analyses clearly demonstrated that, on ASC-EV treatment, an increased number of capillary/number of muscle fiber are present in the

ischemic muscles. Moreover, concerns could be also raised by the protocol we adopted, owing to the minimal residual blood flow (10%) detected after surgery (see Figure III in the online-only Data Supplement). However, based on our results, it can be speculated that intravenous ASC-EVs administration at T0, may have dual beneficial effects: locally, to boost of a hasty angiogenic response, systemically, to activate signals in circulating inflammatory cells impairing their recruitment into ischemic tissues, and prevent damage. Finally, since a low residual blood flow is a common feature in critical limb ischemia patients undergoing revascularization, it could be speculated that this protocol might be beneficial even in clinical settings.

ARTICLE INFORMATION

Received August 3, 2019; accepted October 17, 2019.

Affiliations

From the 2i3T Scarl University of Turin (F.F., M.C., C.C.), University of Turin, Italy. Department of Medical Sciences (A. Ranghino, C.G., M.T., A. Rossi, G.T., S.F., M.V.G., G.C., M.F.B.), University of Turin, Italy.

Sources of Funding

This work was supported by grant number 071215 from Unicyte to 2i3T to G. Camussi and M.F. Brizzi. Associazione Italiana per la Ricerca sul Cancro (AIRC) project IG 2015.17630 to M.F. Brizzi.

Disclosures

G. Camussi is a component of the Scientific Advisory Board of Unicyte AG. The other authors report no conflicts.

REFERENCES

1. Olin, JW, White, CJ, Armstrong, EJ, Kadian-Dodov, D, Hiatt, WR. Peripheral artery disease. *N Engl J Med*. 2016;67:558–587.
2. Vartanian, SM, Conte, MS. Surgical intervention for peripheral arterial disease. *Circ Res*. 2015;116:1614–1628. doi: 10.1161/CIRCRESAHA.116.303504 Crossref. PubMed.
3. Thukkani, AK, Kinlay, S. Endovascular intervention for peripheral artery disease. *Circ Res*. 2015;116:1599–1613. doi: 10.1161/CIRCRESAHA.116.303503 Crossref. PubMed.
4. Gupta, NK, Armstrong, EJ, Parikh, SA. The current state of stem cell therapy for peripheral artery disease. *Curr Cardiol Rep*. 2014;16:447. doi: 10.1007/s11886-013-0447-2 Crossref. PubMed.
5. Vizoso, FJ, Eiro, N, Cid, S, Schneider, J, Perez-Fernandez, R. Mesenchymal stem cell secretome: toward cell-free therapeutic strategies in regenerative medicine. *Int J Mol Sci*. 2017;18:E1852. Crossref. PubMed.
6. Bronckaers, A, Hilkens, P, Martens, W, Gervois, P, Ratajczak, J, Struys, T, Lambrichts, I. Mesenchymal stem/stromal cells as a pharmacological and therapeutic approach to accelerate angiogenesis. *Pharmacol Ther*. 2014;143:181–196. doi: 10.1016/j.pharmthera.2014.02.013 Crossref. PubMed.
7. Camussi, G. Stem cell reviews and reports: microenvironment and extracellular microvesicles section. *Stem Cell Rev Rep*. 2017;13:4. doi: 10.1007/s12015-017-9725-5 Crossref. PubMed.
8. Lee, Y, El Andaloussi, S, Wood, MJ. Exosomes and microvesicles: extracellular vesicles for genetic information transfer and gene therapy. *Hum Mol Genet*. 2012;21(R1):R125–R134. doi: 10.1093/hmg/dds317 Crossref. PubMed.
9. Liu, L, Jin, X, Hu, CF, Li, R, Zhou, Z, Shen, CX. Exosomes derived from mesenchymal stem cells rescue myocardial ischaemia/ reperfusion injury by inducing cardiomyocyte autophagy via AMPK and Akt

pathways. *Cell Physiol Biochem*. 2017;43:52–68. doi: 10.1159/000480317 Crossref. PubMed.

10. Herrera, MB, Fonsato, V, Gatti, S, Deregibus, MC, Sordi, A, Cantarella, D, Calogero, R, Bussolati, B, Tetta, C, Camussi, G. Human liver stem cell-derived microvesicles accelerate hepatic regeneration in hepatectomized rats. *J Cell Mol Med*. 2010;14(6B):1605–1618. doi: 10.1111/j.1582-4934.2009.00860.x Crossref. PubMed.
11. Jones, NC, Tyner, KJ, Nibarger, L, Stanley, HM, Cornelison, DD, Fedorov, YV, Olwin, BB. The p38alpha/beta MAPK functions as a molecular switch to activate the quiescent satellite cell. *J Cell Biol*. 2005;169:105–116. doi: 10.1083/jcb.200408066 Crossref. PubMed.
12. Zhao, L, Johnson, T, Liu, D. Therapeutic angiogenesis of adipose-derived stem cells for ischemic diseases. *Stem Cell Res Ther*. 2017;8:125. doi: 10.1186/s13287-017-0578-2 Crossref. PubMed.
13. Cavallari, C, Ranghino, A, Tapparo, M, Cedrino, M, Figliolini, F, Grange, C, Giannachi, V, Garneri, P, Deregibus, MC, Collino, F, et al. Serum-derived extracellular vesicles (EVs) impact on vascular remodeling and prevent muscle damage in acute hind limb ischemia. *Sci Rep*. 2017;7:8180. doi: 10.1038/s41598-017-08250-0 Crossref. PubMed.
14. Ranghino, A, Cantaluppi, V, Grange, C, Vitillo, L, Fop, F, Biancone, L, Deregibus, MC, Tetta, C, Segoloni, GP, Camussi, G. Endothelial progenitor cell-derived microvesicles improve neovascularization in a murine model of hindlimb ischemia. *Int J Immunopathol Pharmacol*. 2012;25:75–85. doi: 10.1177/039463201202500110 Crossref. PubMed.
15. Togliatto, G, Trombetta, A, Dentelli, P, Cotogni, P, Rosso, A, Tschöp, MH, Granata, R, Ghigo, E, Brizzi, MF. Unacylated ghrelin promotes skeletal muscle regeneration following hindlimb ischemia via SOD-2-mediated miR-221/222 expression. *J Am Heart Assoc*. 2013;2:e000376. doi: 10.1161/JAHA.113.000376 Crossref. PubMed.
16. Penna, C, Tullio, F, Femminò, S, Rocca, C, Angelone, T, Cerra, MC, Gallo, MP, Gesmundo, I, Fanciulli, A, Brizzi, MF, et al. Obestatin regulates cardiovascular function and promotes cardioprotection through the nitric oxide pathway. *J Cell Mol Med*. 2017;21:3670–3678. doi: 10.1111/jcmm.13277 Crossref. PubMed.
17. Deregibus, MC, Figliolini, F, D'Antico, S, Manzini, PM, Pasquino, C, De Lena, M, Tetta, C, Brizzi, MF, Camussi, G. Charge-based precipitation of extracellular vesicles. *Int J Mol Med*. 2016;38:1359–1366. doi: 10.3892/ijmm.2016.2759 Crossref. PubMed.
18. Benito-Martin, A, Peinado, H. FunRich proteomics software analysis, let the fun begin! *Proteomics*. 2015;15:2555–2556. doi: 10.1002/pmic.201500260 Crossref. PubMed.
19. Campbell, TL, Mitchell, AS, McMillan, EM, Bloemberg, D, Pavlov, D, Messa, I, Mielke, JG, Quadrilatero, J. High-fat feeding does not induce an autophagic or apoptotic phenotype in female rat skeletal muscle. *Exp Biol Med (Maywood)*. 2015;240:657–668. doi: 10.1177/1535370214557223 Crossref. PubMed.
20. Hirata, M, Sakuma, K, Okajima, S, Fujiwara, H, Inashima, S, Yasuhara, M, Kubo, T. Increased expression of neuregulin-1 in differentiating muscle satellite cells and in motoneurons during muscle regeneration. *Acta Neuropathol*. 2007;113:451–459. doi: 10.1007/s00401-007-0198-5 Crossref. PubMed.
21. Ho, AT Van, Hayashi, S, Bröhl, D, Auradé, F, Rattenbach, R, Relaix, F. Neural crest cell lineage restricts skeletal muscle progenitor cell differentiation through neuregulin1-ErbB3 signaling. *Dev Cell*. 2011;21:273–287. Crossref. PubMed.
22. Hedhli, N, Dobrucki, LW, Kalinowski, A, Zhuang, ZW, Wu, X, Russell, RR 3rd, Sinusas, AJ, Russell, KS. Endothelial-derived neuregulin is an important mediator of ischaemia-induced angiogenesis and arteriogenesis. *Cardiovasc Res*. 2012;93:516–524. doi: 10.1093/cvr/cvr352 Crossref. PubMed.
23. Jacobson, C, Duggan, D, Fischbach, G. Neuregulin induces the expression of transcription factors and myosin heavy chains typical of muscle spindles in cultured human muscle. *Proc Natl Acad Sci U S A*. 2004;101:12218–12223. doi: 10.1073/pnas.0404240101 Crossref. PubMed.
24. Russell, KS, Stern, DF, Polverini, PJ, Bender, JR. Neuregulin activation of ErbB receptors in vascular endothelium leads to angiogenesis. *Am J Physiol*. 1999;277:H2205–H2211. doi:

10.1152/ajpheart.1999.277.6.H2205 PubMed.

25. Lopatina, T, Favaro, E, Grange, C, Cedrino, M, Ranghino, A, Occhipinti, S, Fallo, S, Buffolo, F, Gaykalova, DA, Zanone, MM, et al. PDGF enhances the protective effect of adipose stem cell-derived extracellular vesicles in a model of acute hindlimb ischemia. *Sci Rep*. 2018;8:17458. doi: 10.1038/s41598-018-36143-3 Crossref. PubMed.
26. Ryzhov, S, Matafonov, A, Galindo, CL, Zhang, Q, Tran, TL, Lenihan, DJ, Lenneman, CG, Feoktistov, I, Sawyer, DB. ERBB signaling attenuates proinflammatory activation of nonclassical monocytes. *Am J Physiol Heart Circ Physiol*. 2017;312:H907–H918. doi: 10.1152/ajpheart.00486.2016 Crossref. PubMed.
27. Krishna, SM, Moxon, JV, Golledge, J. A review of the pathophysiology and potential biomarkers for peripheral artery disease. *Int J Mol Sci*. 2015;16:11294–11322. doi: 10.3390/ijms160511294 Crossref. PubMed.
28. Park, JU, Kwon, ST. Potential of autologous adipose-derived stem cells to regenerate atrophied muscle in a rat model. *Wound Repair Regen*. 2017;25:944–955. doi: 10.1111/wrr.12598 Crossref. PubMed.
29. Rybalko, V, Hsieh, PL, Ricles, LM, Chung, E, Farrar, RP, Suggs, LJ. Therapeutic potential of adipose-derived stem cells and macrophages for ischemic skeletal muscle repair. *Regen Med*. 2017;12:153–167. doi: 10.2217/rme-2016-0094 Crossref. PubMed.
30. Camussi, G, Deregibus, MC, Quesenberry, PJ. Role of stem cell-derived extracellular RNA-carrying vesicles cell reprogramming. *Austin J Clin Pathol*. 2014;1:1001.
31. Kang, T, Jones, TM, Naddell, C, Bacanamwo, M, Calvert, JW, Thompson, WE, Bond, VC, Chen, YE, Liu, D. Adipose-derived stem cells induce angiogenesis via microvesicle transport of miRNA-31. *Stem Cells Transl Med*. 2016;5:440–450. doi: 10.5966/sctm.2015-0177 Crossref. PubMed.
32. Lopatina, T, Bruno, S, Tetta, C, Kalinina, N, Porta, M, Camussi, G. Platelet-derived growth factor regulates the secretion of extracellular vesicles by adipose mesenchymal stem cells and enhances their angiogenic potential. *Cell Commun Signal*. 2014;12:26. doi: 10.1186/1478-811X-12-26 Crossref. PubMed.
33. Togliatto, G, Dentelli, P, Gili, M, Gallo, S, Deregibus, C, Biglieri, E, Iavello, A, Santini, E, Rossi, C, Solini, A, et al. Obesity reduces the pro-angiogenic potential of adipose tissue stem cell-derived extracellular vesicles (EVs) by impairing miR-126 content: impact on clinical applications. *Int J Obes (Lond)*. 2016;40:102–111. doi: 10.1038/ijo.2015.123 Crossref. PubMed.
34. Meyer, D, Yamaai, T, Garratt, A, Riethmacher-Sonnenberg, E, Kane, D, Theill, LE, Birchmeier, C. Isoform-specific expression and function of neuregulin. *Development*. 1997;124:3575–3586. PubMed.
35. Britsch, S. The neuregulin-I/ErbB signaling system in development and disease. *Adv Anat Embryol Cell Biol*. 2007;190:1–65. PubMed.
36. Gumà, A, Martínez-Redondo, V, López-Soldado, I, Cantó, C, Zorzano, A. Emerging role of neuregulin as a modulator of muscle metabolism. *Am J Physiol Endocrinol Metab*. 2010;298:E742–E750. doi: 10.1152/ajpendo.00541.2009 Crossref. PubMed.
37. Wang, T, Cunningham, A, Dokun, AO, Hazarika, S, Houston, K, Chen, L, Lye, RJ, Spolski, R, Leonard, WJ, Annex, BH. Loss of interleukin-21 receptor activation in hypoxic endothelial cells impairs perfusion recovery after hindlimb ischemia. *Arterioscler Thromb Vasc Biol*. 2015;35:1218–1225. doi: 10.1161/ATVBAHA.115.305476 Crossref. PubMed.